Published in final edited form as:
Mol Pharm. 2012 August 6; 9(8): 2322–2330. doi:10.1021/mp300246j.

Cu-64-Labeled Lactam Bridge-Cyclized α-MSH Peptides for PET Imaging of Melanoma

Haixun Guo[†] and **Yubin Miao**[*,†,⊥,φ]

[†]College of Pharmacy, University of New Mexico, Albuquerque, NM 87131, USA

[⊥]Cancer Research and Treatment Center, University of New Mexico, Albuquerque, NM 87131, USA

[φ]Department of Dermatology, University of New Mexico, Albuquerque, NM 87131, USA

Abstract

The purpose of this study was to examine and compare the melanoma targeting and imaging properties of ^{64}Cu-NOTA-GGNle-CycMSH$_{hex}$ {^{64}Cu-1,4,7-triazacyclononane-1,4,7-triacetic acid-Gly-Gly-Nle-c[Asp-His-DPhe-Arg-Trp-Lys]-CONH$_2$} and ^{64}Cu-DOTA-GGNle-CycMSH$_{hex}$ {^{64}Cu-1,4,7,10-tetraazacyclononane-1,4,7,10-tetraacetic acid-GGNle-CycMSH$_{hex}$}. Two lactam bridge-cyclized peptides, NOTA-GGNle-CycMSH$_{hex}$ and DOTA-GGNle-CycMSH$_{hex}$, were synthesized using fluorenylmethyloxy carbonyl (Fmoc) chemistry. The melanocortin-1 (MC1) receptor binding affinity of NOTA-GGNle-CycMSH$_{hex}$ was determined in B16/F1 melanoma cells and compared with DOTA-GGNle-CycMSH$_{hex}$. The melanoma targeting and imaging properties of ^{64}Cu-NOTA-GGNle-CycMSH$_{hex}$ and ^{64}Cu-DOTA-GGNle-CycMSH$_{hex}$ were determined in B16/F1 melanoma-bearing C57 mice. NOTA-GGNle-CycMSH$_{hex}$ and DOTA-GGNle-CycMSH$_{hex}$ displayed comparable MC1 receptor binding affinities (1.6 vs. 2.1 nM). The substitution of DOTA with NOTA dramatically increased the melanoma uptake and decreased the renal and liver uptake of ^{64}Cu-NOTA-GGNle-CycMSH$_{hex}$. The tumor uptake of ^{64}Cu-NOTA-GGNle-CycMSH$_{hex}$ was between 12.39 ± 1.61 and 12.71 ± 2.68 % ID/g at 0.5, 2 and 4 h post-injection. The accumulation of ^{64}Cu-NOTA-GGNle-CycMSH$_{hex}$ activity in normal organs was lower than 1.02 % ID/g except for the kidneys 2, 4 and 24 h post-injection. The tumor/liver uptake ratios of ^{64}Cu-NOTA-GGNle-CycMSH$_{hex}$ were 17.96, 16.95 and 8.02, whereas the tumor/kidney uptake ratios of ^{64}Cu-NOTA-GGNle-CycMSH$_{hex}$ were 2.52, 3.60 and 5.74 at 2, 4 and 24 h post-injection, respectively. Greater than 91% of the injected radioactivity cleared through the urinary system by 2 h post-injection. The substitution of DOTA with NOTA resulted in a dramatic increase in melanoma uptake and decrease in renal and liver uptake of ^{64}Cu-NOTA-GGNle-CycMSH$_{hex}$ compared to ^{64}Cu-DOTA-GGNle-CycMSH$_{hex}$. High melanoma uptake coupled with low accumulation in non-target organs suggested ^{64}Cu-NOTA-GGNle-CycMSH$_{hex}$ as a lead radiolabeled peptide for melanoma imaging and therapy.

Keywords

Alpha-melanocyte stimulating hormone; ^{64}Cu-labeled peptide; lactam bridge-cyclized peptide; positron emission tomography; melanoma imaging

Corresponding Author: Yubin Miao, 2502 Marble NE, MSC09 5360, College of Pharmacy, University of New Mexico, Albuquerque, NM 87131, USA. Phone: (505) 925-4437; Fax: (505) 272-6749; ymiao@salud.unm.edu.

INTRODUCTION

Melanoma is the most deadly skin cancer with an increased incidence worldwide over the past decade. The cancer statistics from the American Cancer Society predicted that 68,130 new melanoma cases would be diagnosed and 8,700 deaths of melanoma would occur in 2010 in the United States.[1] There is a great need for better diagnostic strategies and more effective treatments for melanoma since no curative treatment exists for patients with metastatic melanoma. At the present time, the utilization of melanocortin-1 (MC1) receptor-targeting radiolabeled alpha-melanocyte stimulating hormone (α-MSH) peptides represents a very promising strategy for melanoma detection and treatment. This strategy takes advantage of fast distribution via blood circulation, receptor-targeting cancer tissue localization and rapid whole-body clearance of the radiolabeled α-MSH peptides. Both linear and cyclized α-MSH peptide radiopharmaceuticals have been reported to target the MC1 receptors[2–6] for melanoma imaging and therapy.[7–23]

Over the past several years, we have developed two generations of novel lactam bridge-cyclized ^{111}In-labeled α-MSH peptides for melanoma imaging using single photon emission computed tomography (SPECT).[18–23] The first-generation peptides built upon the backbone of CycMSH {c[Lys-Nle-Glu-His-DPhe-Arg-Trp-Gly-Arg-Pro-Val-Asp], 12 amino acids} peptide,[18–21] whereas the second-generation peptides were based on the construct of $CycMSH_{hex}$ {c[Asp-His-DPhe-Arg-Trp-Lys]-$CONH_2$, 6 amino acids} peptide. [22–23] The MC1 receptor binding motif (His-DPhe-Arg-Trp) was retained in the 12-amino acid CycMSH moiety cyclized by a Lys-Asp lactam bridge, or in the 6-amino acid $CycMSH_{hex}$ moiety cyclized via an Asp-Lys lactam bridge. The radiometal chelator DOTA (1,4,7,10-Tetraazacyclododecane-1,4,7,10-tetraacetic acid) was conjugated to the *N*-terminus of the CycMSH or $CycMSH_{hex}$ moiety with or without an amino acid linker for radiolabeling. The second-generation ^{111}In-labeled $CycMSH_{hex}$ peptides exhibited enhanced melanoma uptake and reduced renal uptake than the first-generation ^{111}In-labeled CycMSH peptides.[18–23] For instance, ^{111}In-DOTA-Nle-$CycMSH_{hex}$ displayed higher melanoma uptake (19.39 ± 1.65 % ID/g at 2 h post-injection) and lower renal uptake (9.52 ± 0.44 % ID/g at 2 h post-injection) compared to ^{111}In-DOTA-GlyGlu-CycMSH in B16/F1 melanoma-bearing C57 mice.[18–22] Recently, we have found that the introduction of the -GlyGly- linker between the DOTA and Nle-$CycMSH_{hex}$ moiety maintained high melanoma uptake (19.05 ± 5.04 % ID/g at 2 h post-injection) while reducing the renal and liver uptake of ^{111}In-DOTA-GGNle-$CycMSH_{hex}$ by 42 and 68% compared to ^{111}In-DOTA-Nle-$CycMSH_{hex}$.[23] The melanoma lesions could be clearly visualized by SPECT/CT using ^{111}In-DOTA-GGNle-$CycMSH_{hex}$ as an imaging probe.[23]

We have been interested in expanding our melanoma imaging modality from SPECT to positron emission tomography (PET) because PET has some distinct advantages over other functional imaging modalities in terms of sensitivity, resolution and quantification. The combination of the outstanding imaging properties of PET with specific receptor-targeting properties of peptide radiopharmaceuticals offers an exciting opportunity for sensitive tumor-specific imaging. Copper-64 ($t_{1/2}$=12.7 h, 17.4% β^+, 40% β^-) is an attractive PET radionuclide coupled with therapeutic properties due to its positron- and electron-emissions.[24–26] Despite the fact that DOTA can form stable complexes with a variety of diagnostic and therapeutic radionuclides, DOTA can only form a moderately stable complex with ^{64}Cu due to the demetallation of ^{64}Cu-DOTA moiety *in vivo*. The dissociation of ^{64}Cu from DOTA chelator generally resulted in high accumulation in non-target tissues such as liver.[13,15,27–30] Alternatively, 1,4,7-triazacyclononane-1,4,7-triacetic acid (NOTA) could form a more stable complex with ^{64}Cu than DOTA *in vivo*. It was reported that the ^{64}Cu-NOTA-8-Aoc-BBN(7-14)NH_2 displayed higher resistance to transmetallation reactions *in vivo* than ^{64}Cu-DOTA-8-Aoc-BBN(7-14)NH_2.[27] ^{64}Cu-NOTA-8-Aoc-BBN(7-14)NH_2

displayed considerably lower liver uptake than ^{64}Cu-DOTA-8-Aoc-BBN(7-14)NH_2[27,28] in PC-3 tumor-bearing mice, underscoring the advantage of NOTA for ^{64}Cu conjugation compared to DOTA.

^{111}In-DOTA-GGNle-CycMSH$_{hex}$ exhibited more favorable pharmacokinetic properties (comparable high tumor uptake, less renal and liver uptake) than ^{111}In-DOTA-Nle-CycMSH$_{hex}$ in our previous reports.[22,23] Hence, we managed to develop PET imaging probes building upon the GGNle-CycMSH$_{hex}$ peptide construct. In this study, we hypothesized that ^{64}Cu-NOTA-GGNle-CycMSH$_{hex}$ would display more favorable melanoma targeting and pharmacokinetic properties than ^{64}Cu-DOTA-GGNle-CycMSH$_{hex}$. To examine the hypothesis, we synthesized NOTA-GGNle-CycMSH$_{hex}$ and DOTA-GGNle-CycMSH$_{hex}$ peptides. The MC1 receptor binding affinity of NOTA-GGNle-CycMSH$_{hex}$ was determined in B16/F1 melanoma cells and compared with DOTA-GGNle-CycMSH$_{hex}$. Thereafter, we examined the biodistribution properties of ^{64}Cu-NOTA-GGNle-CycMSH$_{hex}$ and ^{64}Cu-DOTA-GGNle-CycMSH$_{hex}$ in B16/F1 melanoma-bearing C57 mice. Furthermore, we determined the melanoma imaging properties of ^{64}Cu-NOTA-GGNle-CycMSH$_{hex}$ and ^{64}Cu-DOTA-GGNle-CycMSH$_{hex}$ in B16/F1 melanoma-bearing C57 mice using small animal PET/CT.

EXPERIMENTAL SECTION

Chemicals and Reagents

Amino acid and resin were purchased from Advanced ChemTech Inc. (Louisville, KY) and Novabiochem (San Diego, CA). NO2AtBu ester was purchased from CheMatech Inc. (Dijon, France) for peptide synthesis. ^{125}I-Tyr^2-[Nle^4, D-Phe^7]-α-MSH {^{125}I-(Tyr^2)-NDP-MSH} was obtained from PerkinElmer, Inc. (Waltham, MA) for receptor binding assay. $^{64}CuCl_2$ was purchased from Trace Life Sciences, Inc. (Dallas, TX) for radiolabeling. All other chemicals used in this study were purchased from Thermo Fischer Scientific (Waltham, MA) and used without further purification. B16/F1 murine melanoma cells were obtained from American Type Culture Collection (Manassas, VA).

Peptide Synthesis and Receptor Binding Assay

New NOTA-GGNle-CycMSH$_{hex}$ was synthesized using fluorenylmethyloxy carbonyl (Fmoc) chemistry. Briefly, the intermediate scaffold of Fmoc-Asp(O-2-PhiPr)-His(Trt)-DPhe-Arg(Pbf)-Trp(Boc)-Lys(Mtt) was synthesized on H_2N-Novagel resin by an Advanced ChemTech multiple-peptide synthesizer (Louisville, KY). Generally, 70 μmol of resin, 210 μmol of each Fmoc-protected amino acid and NO2AtBu were used for the synthesis. The protecting groups of Mtt and 2-phenylisopropyl were removed by 2.5% of trifluoroacetic acid (TFA) for peptide cyclization. The cyclization reaction was achieved on the resin by an overnight reaction in *N*,*N*-dimethylformamide (DMF) using benzotriazole-1-yl-oxy-tris-pyrrolidino-phosphonium-hexafluorophosphate (PyBOP) as a coupling agent in the presence of *N*,*N*-diisopropylethylamine (DIPEA). After the cyclization, the moiety of NO2AtBu-CH_2-Gly-Gly-Nle was coupled to the cyclic intermediate scaffold to yield NO2AtBu-CH_2-Gly-Gly-Nle-Cyclic[Asp-His(Trt)-DPhe-Arg(Pbf)-Trp(Boc)-Lys] on the resin. All protecting groups were totally removed and the peptide was cleaved from the resin by treating with a mixture of trifluoroacetic acid (TFA), thioanisole, phenol, water, ethanedithiol and triisopropylsilane (87.5:2.5:2.5:2.5:2.5:2.5) for 2 h at 25 °C. The peptide was precipitated and washed with ice-cold ether four times, purified by reverse phase-high performance liquid chromatography (RP-HPLC) and characterized by liquid chromatography-mass spectrometry (LC-MS). DOTA-GGNle-CycMSH$_{hex}$ was synthesized, purified by RP-HPLC and characterized by LC-MS according to our published procedure.[23] The MC1 receptor binding affinity (IC_{50} value) of NOTA-GGNle-CycMSH$_{hex}$ was

determined in B16/F1 melanoma cells by *in vitro* competitive receptor binding assay according to our published procedure.[23] The IC_{50} value of DOTA-GGNle-CycMSH$_{hex}$ was cited from our previous report[23] for direct comparison.

Peptide Radiolabeling with ^{64}Cu

Both ^{64}Cu-NOTA-GGNle-CycMSH$_{hex}$ and ^{64}Cu-DOTA-GGNle-CycMSH$_{hex}$ were prepared in a 0.5 M NH_4OAc-buffered solution at pH 5.4. Briefly, 10 μL of $^{64}CuCl_2$ (37–74 MBq in 0.05 M HCl aqueous solution), 10 μL of 1 mg/mL NOTA-GGNle-CycMSH$_{hex}$ or DOTA-GGNle-CycMSH$_{hex}$ aqueous solution and 200 μL of 0.5 M NH_4OAc (pH 5.4) were added into a reaction vial and incubated at 75 °C for 1 h. After the incubation, 10 μL of 0.5% EDTA aqueous solution was added into the reaction vial to scavenge potential unbound $^{64}Cu^{2+}$ ions. The radiolabeled complexes were purified to single species by Waters RP-HPLC (Milford, MA) on a Grace Vydac C-18 reverse phase analytical column (Deerfield, IL) using a 20-minute gradient of 18–28% acetonitrile in 20 mM HCl aqueous solution with a flow rate of 1.0 mL/min. Each purified peptide sample was purged with N_2 gas at 25 °C for 20 min to remove the acetonitrile. The pH of final solution was adjusted to 7.4 with 0.1 N NaOH and sterile normal saline for animal studies. *In vitro* serum stabilities of both ^{64}Cu-NOTA-GGNle-CycMSH$_{hex}$ and ^{64}Cu-DOTA-GGNle-CycMSH$_{hex}$ were determined by incubation in mouse serum at 37 °C for 2 h and monitored for degradation by RP-HPLC.

Biodistribution Studies

All the animal studies were conducted in compliance with Institutional Animal Care and Use Committee approval. The melanoma targeting and pharmacokinetic properties of ^{64}Cu-NOTA-GGNle-CycMSH$_{hex}$ and ^{64}Cu-DOTA-GGNle-CycMSH$_{hex}$ were determined in B16/F1 melanoma-bearing C57 female mice (Harlan, Indianapolis, IN). The C57 mice were subcutaneously inoculated with 1×10^6 B16/F1 cells on the right flank for each mouse to generate B16/F1 tumors. The weights of tumors reached approximately 0.2 g 10 days post cell inoculation. Each melanoma-bearing mouse was injected with 0.037 MBq of ^{64}Cu-NOTA-GGNle-CycMSH$_{hex}$ or ^{64}Cu-DOTA-GGNle-CycMSH$_{hex}$ via the tail vein. Groups of five mice were sacrificed at 0.5, 2, 4 and 24 h post-injection, and tumors and organs of interest were harvested, weighed and counted. Blood values were taken as 6.5% of the whole-body weight. The specificities of the tumor uptake of ^{64}Cu-NOTA-GGNle-CycMSH$_{hex}$ and ^{64}Cu-DOTA-GGNle-CycMSH$_{hex}$ were determined by co-injecting 10 μg (6.07 nmol) of unlabeled NDP-MSH peptide at 2 h post-injection.

Melanoma Imaging with ^{64}Cu-NOTA-GGNle-CycMSH$_{hex}$ and ^{64}Cu-DOTA-GGNle-CycMSH$_{hex}$

The melanoma imaging properties of ^{64}Cu-NOTA-GGNle-CycMSH$_{hex}$ or ^{64}Cu-DOTA-GGNle-CycMSH$_{hex}$ were determined in B16/F1 melanoma-bearing C57 mice using small animal PET/CT. Approximately 37.0 MBq of ^{64}Cu-NOTA-GGNle-CycMSH$_{hex}$ or ^{64}Cu-DOTA-GGNle-CycMSH$_{hex}$ was injected into each mouse via the tail vein. The mice were sacrificed for small animal PET and CT imaging 2 and 4 h post-injection. The 9-min CT imaging performed by Nano-SPECT/CT (Bioscan, Washington DC) was immediately followed by the PET imaging conducted by LabPET (Gamma Media-Ideas, Quebec, Canada) using the same animal bed. The PET data were reconstructed by maximum-likelihood expectation maximization (MLEM) reconstruction algorithms. The CT data were reconstructed, visualized and fused with the PET data using InVivoScope (Bioscan, Washington DC).

Statistical Analysis

Statistical analysis was performed using the Student's t-test for unpaired data. A 95% confidence level was chosen to determine the significance of the difference in tumor, kidney and liver uptake between ^{64}Cu-NOTA-GGNle-CycMSH$_{hex}$ with/without NDP-MSH co-injection, and between ^{64}Cu-DOTA-GGNle-CycMSH$_{hex}$ with/without NDP-MSH co-injection. The differences at the 95% confidence level ($p<0.05$) were considered significant.

RESULTS

Novel NOTA-GGNle-CycMSH$_{hex}$ was synthesized and purified by RP-HPLC. NOTA-GGNle-CycMSH$_{hex}$ displayed greater than 90% chemical purity after HPLC purification. The identity of NOTA-GGNle-CycMSH$_{hex}$ was confirmed by electrospray ionization mass spectrometry. The calculated and found molecular weights of NOTA-GGNle-CycMSH$_{hex}$ were 1381 and 1381, respectively. Meanwhile, DOTA-GGNle-CycMSH$_{hex}$ was synthesized and characterized according to our published procedure[23] for direct comparison. The schematic structures of NOTA-GGNle-CycMSH$_{hex}$ and DOTA-GGNle-CycMSH$_{hex}$ are shown in Figure 1. The competitive binding curve of NOTA-GGNle-CycMSH$_{hex}$ in B16/F1 cells is presented in Figure 2 and compared with DOTA-GGNle-CycMSH$_{hex}$. The IC_{50} of NOTA-GGNle-CycMSH$_{hex}$ was 1.6 nM, which was comparable to that of DOTA-GGNle-CycMSH$_{hex}$ (2.1 nM).[23]

Both NOTA-GGNle-CycMSH$_{hex}$ and DOTA-GGNle-CycMSH$_{hex}$ were readily labeled with ^{64}Cu in 0.5 M ammonium acetate at pH 5.4 with greater than 95% radiolabeling yields. ^{64}Cu-NOTA-GGNle-CycMSH$_{hex}$ and ^{64}Cu-DOTA-GGNle-CycMSH$_{hex}$ were completely separated from their excess non-labeled peptides by RP-HPLC. The specific activities of ^{64}Cu-NOTA-GGNle-CycMSH$_{hex}$ and ^{64}Cu-DOTA-GGNle-CycMSH$_{hex}$ were approximately 20,000 Ci/g and 20,000 Ci/g, respectively. The retention times of ^{64}Cu-NOTA-GGNle-CycMSH$_{hex}$ and ^{64}Cu-DOTA-GGNle-CycMSH$_{hex}$ were 18.5 and 18.8 min, respectively. Both ^{64}Cu-NOTA-GGNle-CycMSH$_{hex}$ and ^{64}Cu-DOTA-GGNle-CycMSH$_{hex}$ showed greater than 98% radiochemical purities after HPLC purification, and were stable in mouse serum at 37°C for 2 h. Only intact ^{64}Cu-NOTA-GGNle-CycMSH$_{hex}$ and ^{64}Cu-DOTA-GGNle-CycMSH$_{hex}$ were detected by RP-HPLC after 2 h of incubation in mouse serum.

The melanoma targeting and pharmacokinetic properties of ^{64}Cu-NOTA-GGNle-CycMSH$_{hex}$ and ^{64}Cu-DOTA-GGNle-CycMSH$_{hex}$ were determined in B16/F1 melanoma-bearing C57 mice. The biodistribution results of ^{64}Cu-NOTA-GGNle-CycMSH$_{hex}$ and ^{64}Cu-DOTA-GGNle-CycMSH$_{hex}$ are presented in Tables 1 and 2. ^{64}Cu-NOTA-GGNle-CycMSH$_{hex}$ exhibited rapid high melanoma uptake and prolonged tumor retention. The tumor uptake value of ^{64}Cu-NOTA-GGNle-CycMSH$_{hex}$ was 12.51 ± 0.44 % ID/g at 0.5 h post-injection. ^{64}Cu-NOTA-GGNle-CycMSH$_{hex}$ displayed similar high tumor uptake (12.39 ± 1.61 and 12.71 ± 2.68 % ID/g) at 2 and 4 h post-injection. Even at 24 h post-injection, there was 4.25 ± 0.32 % ID/g of ^{64}Cu-NOTA-GGNle-CycMSH$_{hex}$ activity remained in the tumor. Approximately 94.2% of the tumor uptake of ^{64}Cu-NOTA-GGNle-CycMSH$_{hex}$ was blocked by 10 μg (6.07 nmol) of non-radiolabeled NDP-MSH ($p<0.05$) (Figure 3), demonstrating that the tumor uptake was specific and MC1 receptor-mediated. Whole-body clearance of ^{64}Cu-NOTA-GGNle-CycMSH$_{hex}$ was rapid, with 91.7% of the injected radioactivity cleared through the urinary system by 2 h post-injection. Normal organ uptake of ^{64}Cu-NOTA-GGNle-CycMSH$_{hex}$ was lower than 1.02 % ID/g except for the kidneys at 2, 4 and 24 h post-injection. The liver uptake of ^{64}Cu-NOTA-GGNle-CycMSH$_{hex}$ was only 0.69 ± 0.06 and 0.75 ± 0.17 % ID/g at 2 and 4 h post-injection. The kidney uptake was 9.28 ± 0.77 % ID/g at 0.5 h post-injection and decreased to 4.92 ± 1.43 % ID/g at 2 h post-injection. The renal uptake was only 0.74 ± 0.18 % ID/g at 24 h post-injection. Co-injection

of NDP-MSH didn't significantly reduce the renal uptake of ^{64}Cu-NOTA-GGNle-CycMSH$_{hex}$ activity at 2 h post-injection, indicating that the renal uptake was not MC1 receptor-mediated. High tumor uptake and prolonged retention coupled with rapid whole-body clearance resulted in high tumor/blood and high tumor/normal organ uptake ratios achieved as early as 0.5 h post-injection. The tumor/liver uptake ratios of ^{64}Cu-NOTA-GGNle-CycMSH$_{hex}$ were 11.37, 17.96, 16.95 and 8.02 at 0.5, 2, 4 and 24 h post-injection, whereas the tumor/kidney uptake ratios of ^{64}Cu-NOTA-GGNle-CycMSH$_{hex}$ were 1.35, 2.52, 3.60 and 5.74 at 0.5, 2, 4 and 24 h post-injection.

As we anticipated, ^{64}Cu-DOTA-GGNle-CycMSH$_{hex}$ showed lower tumor uptake than ^{64}Cu-NOTA-GGNle-CycMSH$_{hex}$ at 0.5, 2 and 4 h post-injection (Figure 4). The tumor uptake of ^{64}Cu-DOTA-GGNle-CycMSH$_{hex}$ was 5.61 ± 0.91, 5.20 ± 1.28 and 5.25 ± 1.22 % ID/g at 0.5, 2 and 4 h post-injection, respectively. Co-injection of non-radioactive NDP-MSH blocked 47.9% of the tumor uptake at 2 h post-injection ($p<0.05$) (Figure 3), indicating that the partial tumor uptake of ^{64}Cu-DOTA-GGNle-CycMSH$_{hex}$ was MC1 receptor-specific. Besides the lower tumor uptake, ^{64}Cu-DOTA-GGNle-CycMSH$_{hex}$ displayed higher renal uptake than ^{64}Cu-NOTA-GGNle-CycMSH$_{hex}$ at all time points investigated. The renal uptake of ^{64}Cu-DOTA-GGNle-CycMSH$_{hex}$ was 14.44 ± 1.85, 9.30 ± 2.81, 7.45 ± 0.96 and 5.39 ± 0.42 % ID/g at 0.5, 2, 4 and 24 h post-injection, respectively. Co-injection of NDP-MSH didn't significantly reduce the renal uptake of ^{64}Cu-DOTA-GGNle-CycMSH$_{hex}$ activity at 2 h post-injection, indicating that the renal uptake was non-specific. Not surprisingly, ^{64}Cu-DOTA-GGNle-CycMSH$_{hex}$ also displayed higher accumulation than ^{64}Cu-NOTA-GGNle-CycMSH$_{hex}$ in normal organs such as liver, lung, heart and stomach at all the time points investigated. The liver uptake of ^{64}Cu-DOTA-GGNle-CycMSH$_{hex}$ was 11.59 ± 1.77, 10.30 ± 1.18, 9.61 ± 1.34 and 7.23 ± 0.58 % ID/g at 0.5, 2, 4 and 24 h post-injection, respectively. High liver uptake associated with ^{64}Cu-DOTA-GGNle-CycMSH$_{hex}$ activity was not receptor-mediated because co-injection of NDP-MSH didn't significantly reduce the liver uptake of ^{64}Cu-DOTA-GGNle-CycMSH$_{hex}$ at 2 h post-injection (Figure 3). In comparison with ^{64}Cu-NOTA-GGNle-CycMSH$_{hex}$, ^{64}Cu-DOTA-GGNle-CycMSH$_{hex}$ exhibited dramatically lower tumor/kidney and tumor/liver uptake ratios (Figure 5) due to the decreased tumor uptake and increased renal and liver uptake. The tumor/kidney uptake ratios of ^{64}Cu-DOTA-GGNle-CycMSH$_{hex}$ were 0.39, 0.56, 0.70 and 1.11 at 0.5, 2, 4 and 24 h post-injection, whereas the tumor/liver uptake ratios of ^{64}Cu-DOTA-GGNle-CycMSH$_{hex}$ were 0.48, 0.50, 0.55 and 0.82 at 0.5, 2, 4 and 24 h post-injection.

We further evaluated the melanoma imaging properties (melanoma visualization and imaging contrast) of ^{64}Cu-NOTA-GGNle-CycMSH$_{hex}$ and ^{64}Cu-DOTA-GGNle-CycMSH$_{hex}$. The coronal and transversal PET/CT images are presented in Figure 6. The melanoma tumors were clearly visualized by PET/CT using either ^{64}Cu-NOTA-GGNle-CycMSH$_{hex}$ or ^{64}Cu-DOTA-GGNle-CycMSH$_{hex}$ as an imaging probe. However, ^{64}Cu-NOTA-GGNle-CycMSH$_{hex}$ displayed higher tumor uptake and lower non-target organ accumulation compared to ^{64}Cu-DOTA-GGNle-CycMSH$_{hex}$. Both coronal and transversal images of ^{64}Cu-NOTA-GGNle-CycMSH$_{hex}$ exhibited high tumor to normal organ uptake ratios except for the kidneys, which was consistent with the biodistribution results.

DISCUSSION

Both ^{64}Cu-labeled DOTA-conjugated linear or rhenium-cyclized a-MSH peptides have been reported to target the MC1 receptors for successful melanoma imaging.[13,15] However, the rhenium-cyclized ^{64}Cu-DOTA-ReCCMSH(Arg^{11}) {^{64}Cu-DOTA-Re-[Cys^{3,4,10}, D-Phe^{7}, Arg^{11}]a-MSH$_{3–13}$}[13] showed higher melanoma uptake than the linear ^{64}Cu-DOTA-NAPamide {Ac-Nle-Asp-His-D-Phe-Arg-Trp-Gly-Lys(^{64}Cu-DOTA)-NH$_2$}[15] at 2, 4 and 24

h post-injection. The melanoma uptake (8.80 ± 1.70 % ID/g) of ^{64}Cu-DOTA-ReCCMSH(Arg^{11}) was 1.9 times the melanoma uptake (4.63 ± 0.45 % ID/g) of ^{64}Cu-DOTA-NAPamide at 2 h post-injection. Not surprisingly, both ^{64}Cu-DOTA-ReCCMSH(Arg^{11}) and ^{64}Cu-DOTA-NAPamide displayed high liver uptake (7.3 vs. 11.0 % ID/g at 2 h post-injection) that could be attributed to the demetallation of ^{64}Cu from the DOTA chelator *in vivo*. The *in vivo* stability of ^{64}Cu-DOTA moiety was dramatically improved by using the CBTE2A {4,11-bis(carboxymethyl)-1,4,8,11-tetraazabicyclo[6.6.2]hexadecane} chelator. Compared to ^{64}Cu-DOTA-ReCCMSH(Arg^{11}), ^{64}Cu-CBTE2A-ReCCMSH(Arg^{11}) showed dramatically reduced liver uptake (1.57 ± 0.42 % ID/g) while maintained similar melanoma uptake (7.09 ± 3.20 % ID/g) at 2 h post-injection.[14] Interestingly, the substitution of DOTA with NOTA considerably reduced the liver uptake of ^{64}Cu-NOTA-8-Aoc-BBN(7-14)NH$_2$ compared to ^{64}Cu-DOTA-8-Aoc-BBN(7-14)NH$_2$ in PC-3 tumor-bearing mice,[27,28] suggesting that the NOTA was more suitable than DOTA for ^{64}Cu conjugation. Therefore, based on the novel GGNle-CycMSH$_{hex}$ peptide construct we identified,[23] we were interested in examining whether the replacement of DOTA with NOTA could enhance the melanoma uptake and reduce the liver uptake of ^{64}Cu-NOTA-GGNle-CycMSH$_{hex}$ compared to ^{64}Cu-DOTA-GGNle-CycMSH$_{hex}$ in this study.

In this study, we hypothesized that ^{64}Cu-NOTA-GGNle-CycMSH$_{hex}$ would display more favorable melanoma targeting and pharmacokinetic properties than ^{64}Cu-DOTA-GGNle-CycMSH$_{hex}$. To examine the hypothesis, we evaluated NOTA-GGNle-CycMSH$_{hex}$ and DOTA-GGNle-CycMSH$_{hex}$ both *in vitro* and *in vivo*. The substitution of DOTA with NOTA slightly improved the MC1 receptor binding affinity of the peptide in B16/F1 melanoma cells (Figure 2). NOTA-GGNle-CycMSH$_{hex}$ exhibited 1.6 nM MC1 receptor binding affinity, whereas DOTA-GGNle-CycMSH$_{hex}$ showed 2.1 nM MC1 receptor binding affinity. Despite the slightly difference in receptor binding affinity between NOTA-GGNle-CycMSH$_{hex}$ and DOTA-GGNle-CycMSH$_{hex}$, we observed dramatic differences in melanoma targeting and pharmacokinetic properties between their ^{64}Cu-conjugates. ^{64}Cu-NOTA-GGNle-CycMSH$_{hex}$ exhibited higher melanoma uptake than ^{64}Cu-DOTA-GGNle-CycMSH$_{hex}$ in B16/F1 melanoma-bearing mice. The tumor uptake of ^{64}Cu-NOTA-GGNle-CycMSH$_{hex}$ was 2.2, 2.4 and 2.4 times the tumor uptake of ^{64}Cu-DOTA-GGNle-CycMSH$_{hex}$ at 0.5, 2 and 4 h post-injection, respectively (Tables 1 and 2, Figure 4). The lower melanoma uptake of ^{64}Cu-DOTA-GGNle-CycMSH$_{hex}$ was likely due to the dissociation of ^{64}Cu from the DOTA chelator *in vivo*. Interestingly, the co-injection of 10 μg of NDP-MSH blocked 94.2% of the tumor uptake of ^{64}Cu-NOTA-GGNle-CycMSH$_{hex}$, whereas the co-injection of 10 μg of NDP-MSH only blocked 47.9% of the tumor uptake of ^{64}Cu-DOTA-GGNle-CycMSH$_{hex}$ (Figure 3). ^{64}Cu-DOTA-GGNle-CycMSH$_{hex}$ showed 2.71 ± 0.42 % ID/g of non-specific melanoma uptake, which was similar to those of ^{64}Cu-DOTA-ReCCMSH(Arg^{11}) and ^{64}Cu-DOTA-NAPamide.[13,15]

The substitution of DOTA with NOTA dramatically reduced the renal uptake of ^{64}Cu-NOTA-GGNle-CycMSH$_{hex}$ compared to ^{64}Cu-DOTA-GGNle-CycMSH$_{hex}$ (Figure 4). The renal uptake of ^{64}Cu-NOTA-GGNle-CycMSH$_{hex}$ was only 64.3%, 52.9%, 47.3% and 13.7% of the renal uptake of ^{64}Cu-DOTA-GGNle-CycMSH$_{hex}$ at 0.5, 2, 4 and 24 h post-injection, respectively. The increased tumor uptake and decreased renal uptake dramatically improved the tumor to kidney uptake ratios of ^{64}Cu-NOTA-GGNle-CycMSH$_{hex}$ at all time points investigated in this study (Figure 5). The tumor to kidney uptake ratios of ^{64}Cu-NOTA-GGNle-CycMSH$_{hex}$ were 3.5, 4.5, 5.1 and 5.2 times those of ^{64}Cu-DOTA-GGNle-CycMSH$_{hex}$ at 0.5, 2, 4 and 24 h post-injection, respectively. Meanwhile, the substitution of DOTA with NOTA dramatically reduced the liver uptake by 14-fold to 0.69 ± 0.06 % ID/g at 2 h post-injection. The liver uptake of ^{64}Cu-NOTA-GGNle-CycMSH$_{hex}$ was lower than 0.8 % ID/g after 2 h post-injection. The liver uptake of ^{64}Cu-NOTA-GGNle-CycMSH$_{hex}$

was only 9.5%, 6.7%, 7.8% and 7.3% of the liver uptake of ^{64}Cu-DOTA-GGNle-CycMSH$_{hex}$ at 0.5, 2, 4 and 24 h post-injection, respectively (Figure 4). Higher tumor uptake and lower liver uptake dramatically enhanced the tumor to liver uptake ratios of ^{64}Cu-NOTA-GGNle-CycMSH$_{hex}$ at all time points investigated in this study (Figure 5). The tumor to liver uptake ratios of ^{64}Cu-NOTA-GGNle-CycMSH$_{hex}$ were 23.7, 35.9, 30.8 and 9.8 times those of ^{64}Cu-DOTA-GGNle-CycMSH$_{hex}$ at 0.5, 2, 4 and 24 h post-injection, respectively. Extremely low liver uptake of ^{64}Cu-NOTA-GGNle-CycMSH$_{hex}$ indicated the *in vivo* stability of ^{64}Cu-NOTA moiety in ^{64}Cu-NOTA-GGNle-CycMSH$_{hex}$ peptide, which was consistent with the findings reported for ^{64}Cu-NOTA-8-Aoc-BBN(7-14)NH$_2$[27,28] and ^{64}Cu-NOTA-STh peptides.[29] As we anticipated, the improved *in vivo* stability of ^{64}Cu-NOTA-GGNle-CycMSH$_{hex}$ also resulted in its low accumulation (<1.02 % ID/g) in non-target organs such as lung, stomach and heart after 2 h post-injection. Rapid whole-body clearance of ^{64}Cu-NOTA-GGNle-CycMSH$_{hex}$ further confirmed its enhanced *in vivo* stability compared to ^{64}Cu-DOTA-GGNle-CycMSH$_{hex}$. Greater than 91% of ^{64}Cu-NOTA-GGNle-CycMSH$_{hex}$ activity cleared out the body through urinary system, whereas only 63% of ^{64}Cu-DOTA-GGNle-CycMSH$_{hex}$ activity excreted out the body via urinary system at 2 h post-injection.

At the present time, ^{64}Cu-CBTE2A-ReCCMSH(Arg^{11}) displayed the highest tumor/kidney ratio (1.11 at 24 h post-injection) and tumor/liver uptake ratio (4.52 at 2 h post-injection) among all reported ^{64}Cu-labeled linear and cyclic a-MSH peptides.[13–15] Remarkably, ^{64}Cu-NOTA-GGNle-CycMSH$_{hex}$ displayed higher tumor uptake and lower renal and liver uptake than ^{64}Cu-CBTE2A-ReCCMSH(Arg^{11}) at all time points investigated in this study. The tumor uptake of ^{64}Cu-NOTA-GGNle-CycMSH$_{hex}$ were 1.5, 1.7 and 1.7 times the tumor uptake of ^{64}Cu-CBTE2A-ReCCMSH(Arg^{11}) at 0.5, 2 and 4 h post-injection. The tumor/kidney uptake ratios of ^{64}Cu-NOTA-GGNle-CycMSH$_{hex}$ were 2.0, 4.5, 3.4 and 5.2 times the tumor/kidney uptake ratios of ^{64}Cu-CBTE2A-ReCCMSH(Arg^{11}) at 0.5, 2, 4 and 24 h post-injection, whereas The tumor/liver uptake ratios of ^{64}Cu-NOTA-GGNle-CycMSH$_{hex}$ were 3.1, 4.0, 4.1 and 2.0 times the tumor/liver uptake ratios of ^{64}Cu-CBTE2A-ReCCMSH(Arg^{11}) at 0.5, 2, 4 and 24 h post-injection (Figure 5). The increase in tumor uptake and decrease in renal and liver uptake of ^{64}Cu-NOTA-GGNle-CycMSH$_{hex}$ were likely due to the structural difference between ^{64}Cu-NOTA-GGNle-CycMSH$_{hex}$ and ^{64}Cu-CBTE2A-ReCCMSH(Arg^{11}). Despite the fact that the melanoma lesions could be visualized by PET/CT using either ^{64}Cu-NOTA-GGNle-CycMSH$_{hex}$ or ^{64}Cu-DOTA-GGNle-CycMSH$_{hex}$ as an imaging probe, ^{64}Cu-NOTA-GGNle-CycMSH$_{hex}$ exhibited higher tumor imaging contrast than ^{64}Cu-DOTA-GGNle-CycMSH$_{hex}$. Higher melanoma uptake coupled with lower accumulation in normal organs suggested ^{64}Cu-NOTA-GGNle-CycMSH$_{hex}$ as a lead radiolabeled peptide for future melanoma imaging and therapy. From the therapeutic perspective, the enhanced tumor/liver and tumor/kidney uptake ratios of ^{64}Cu-NOTA-GGNle-CycMSH$_{hex}$ would potentially increase the absorbed dose to the tumor while keeping the liver and kidneys safe when treating the melanoma with ^{64}Cu-NOTA-GGNle-CycMSH$_{hex}$ in future studies.

In conclusion, the melanoma targeting and imaging properties of ^{64}Cu-NOTA-GGNle-CycMSH$_{hex}$ and ^{64}Cu-DOTA-GGNle-CycMSH$_{hex}$ were determined in B16/F1 melanoma-bearing C57 mice in this study. The substitution of DOTA with NOTA dramatically increased the melanoma uptake and decreased the renal and liver uptake of ^{64}Cu-NOTA-GGNle-CycMSH$_{hex}$ compared to ^{64}Cu-DOTA-GGNle-CycMSH$_{hex}$. High melanoma uptake coupled with low accumulation in non-target organs suggested ^{64}Cu-NOTA-GGNle-CycMSH$_{hex}$ as a lead radiolabeled peptide for future melanoma imaging and therapy.

Acknowledgments

We thank Drs. Jianquan Yang, Fabio Gallazzi and Mr. Benjamin M. Gershman for their technical assistance. This work was supported in part by the NIH grant NM-INBRE P20RR016480/P20GM103451 and University of New Mexico HSC RAC Award. The image in this article was generated by the Keck-UNM Small Animal Imaging Resource established with funding from the W.M. Keck Foundation and the University of New Mexico Cancer Research and Treatment Center (NIH P30 CA118100).

References

1. Jemal A, Siegel R, Xu J, Ward E. Cancer statistics. CA Cancer J Clin. 2010; 60:277–300. [PubMed: 20610543]
2. Siegrist W, Solca F, Stutz S, Giuffre L, Carrel S, Girard J, Eberle AN. Characterization of receptors for alpha-melanocyte-stimulating hormone on human melanoma cells. Cancer Res. 1989; 49:6352–6358. [PubMed: 2804981]
3. Tatro JB, Reichlin S. Specific receptors for alpha-melanocyte-stimulating hormone are widely distributed in tissues of rodents. Endocrinology. 1987; 121:1900–1907. [PubMed: 2822378]
4. Miao Y, Whitener D, Feng W, Owen NK, Chen J, Quinn TP. Evaluation of the human melanoma targeting properties of radiolabeled alpha-melanocyte stimulating hormone peptide analogues. Bioconjugate Chem. 2003; 14:1177–1184.
5. Miao Y, Owen NK, Whitener D, Gallazzi F, Hoffman TJ, Quinn TP. In vivo evaluation of ^{188}Re-labeled alpha-melanocyte stimulating hormone peptide analogs for melanoma therapy. Int J Cancer. 2002; 101:480–487. [PubMed: 12216078]
6. Chen J, Cheng Z, Hoffman TJ, Jurisson SS, Quinn TP. Melanoma-targeting properties of ^{99m}technetium-labeled cyclic alpha-melanocyte-stimulating hormone peptide analogues. Cancer Res. 2000; 60:5649–5658. [PubMed: 11059756]
7. Chen J, Cheng Z, Owen NK, Hoffman TJ, Miao Y, Jurisson SS, Quinn TP. Evaluation of an ^{111}In-DOTA-rhenium cyclized α-MSH analog: a novel cyclic-peptide analog with improved tumor-targeting properties. J Nucl Med. 2001; 42:1847–1855. [PubMed: 11752084]
8. Froidevaux S, Calame-Christe M, Tanner H, Eberle AN. Melanoma targeting with DOTA-alpha-melanocyte-stimulating hormone analogs: structural parameters affecting tumor uptake and kidney uptake. J Nucl Med. 2005; 46:887–895. [PubMed: 15872364]
9. Froidevaux S, Calame-Christe M, Schuhmacher J, Tanner H, Saffrich R, Henze M, Eberle AN. A Gallium-labeled DOTA-α-melanocyte-stimulating hormone analog for PET imaging of melanoma metastases. J Nucl Med. 2004; 45:116–123. [PubMed: 14734683]
10. Froidevaux S, Calame-Christe M, Tanner H, Sumanovski L, Eberle AN. A novel DOTA-alpha-melanocyte-stimulating hormone analog for metastatic melanoma diagnosis. J Nucl Med. 2002; 43:1699–1706. [PubMed: 12468522]
11. Miao Y, Owen NK, Fisher DR, Hoffman TJ, Quinn TP. Therapeutic efficacy of a ^{188}Re-labeled alpha-melanocyte-stimulating hormone peptide analog in murine and human melanoma-bearing mouse models. J Nucl Med. 2005; 46:121–129. [PubMed: 15632042]
12. Miao Y, Hylarides M, Fisher DR, Shelton T, Moore HA, Wester DW, Fritzberg AR, Winkelmann CT, Hoffman TJ, Quinn TP. Melanoma therapy via peptide-targeted alpha-radiation. Clin Cancer Res. 2005; 11:5616–5621. [PubMed: 16061880]
13. McQuade P, Miao Y, Yoo J, Quinn TP, Welch MJ, Lewis JS. Imaging of melanoma using ^{64}Cu- and ^{86}Y-DOTA-ReCCMSH(Arg11), a cyclized peptide analogue of alpha-MSH. J Med Chem. 2005; 48:2985–2992. [PubMed: 15828837]
14. Wei L, Butcher C, Miao Y, Gallazzi F, Quinn TP, Welch MJ, Lewis JS. Synthesis and biologic evaluation of ^{64}Cu-labeled rhenium-cyclized alpha-MSH peptide analog using a cross-bridged cyclam chelator. J Nucl Med. 2007; 48:64–72. [PubMed: 17204700]
15. Cheng Z, Xiong Z, Subbarayan M, Chen X, Gambhir SS. ^{64}Cu-labeled alpha-melanocyte-stimulating hormone analog for MicroPET imaging of melanocortin 1 receptor expression. Bioconjugate Chem. 2007; 18:765–772.

16. Miao Y, Benwell K, Quinn TP. ^{99m}Tc- and ^{111}In-labeled alpha-melanocyte-stimulating hormone peptides as imaging probes for primary and pulmonary metastatic melanoma detection. J Nucl Med. 2007; 48:73–80. [PubMed: 17204701]

17. Cheng Z, Chen J, Miao Y, Owen NK, Quinn TP, Jurisson SS. Modification of the structure of a metallopeptide: synthesis and biological evaluation of ^{111}In-labeled DOTA-conjugated rhenium-cyclized alpha-MSH analogues. J Med Chem. 2002; 45:3048–3056. [PubMed: 12086490]

18. Miao Y, Gallazzi F, Guo H, Quinn TP. ^{111}In-labeled lactam bridge-cyclized alpha-melanocyte stimulating hormone peptide analogues for melanoma imaging. Bioconjugate Chem. 2008; 19:539–547.

19. Guo H, Shenoy N, Gershman BM, Yang J, Sklar LA, Miao Y. Metastatic melanoma imaging with an ^{111}In-labeled lactam bridge-cyclized alpha-melanocyte-stimulating hormone peptide. Nucl Med Biol. 2009; 36:267–276. [PubMed: 19324272]

20. Guo H, Yang J, Gallazzi F, Prossnitz ER, Sklar LA, Miao Y. Effect of DOTA position on melanoma targeting and pharmacokinetic properties of ^{111}In-labeled lactam bridge-cyclized a-melanocyte stimulating hormone peptide. Bioconjugate Chem. 2009; 20:2162–2168.

21. Guo H, Yang J, Shenoy N, Miao Y. Gallium-67-labeled lactam bridge-cyclized alpha-melanocyte stimulating hormone peptide for primary and metastatic melanoma imaging. Bioconjugate Chem. 2009; 20:2356–2363.

22. Guo H, Yang J, Gallazzi F, Miao Y. Reduction of the ring size of radiolabeled lactam bridge-cyclized alpha-MSH peptide resulting in enhanced melanoma uptake. J Nucl Med. 2010; 51:418–426. [PubMed: 20150256]

23. Guo H, Yang J, Gallazzi F, Miao Y. Effects of the amino acid linkers on melanoma-targeting and pharmacokinetic properties of Indium-111-labeled lactam bridge-cyclized a-MSH peptides. J Nucl Med. 2011; 52:608–616. [PubMed: 21421725]

24. Lewis J, Laforest R, Buettner T, Song S, Fujibayashi Y, Connett J, Welch MJ. Copper-64-diacetyl-bis(N4-methylthiosemicarbazone): an agent for radiotherapy. Proc Natl Acad Sci USA. 2001; 98:1206–1211. [PubMed: 11158618]

25. Anderson CJ, Ferdani R. Copper-64 radiopharmaceuticals for PET imaging of cancer: advances in preclinical and clinical research. Cancer Biother Radiopharm. 2009; 24:379–393. [PubMed: 19694573]

26. Liu Z, Li ZB, Cao Q, Liu S, Wang F, Chen X. Small-animal PET of tumors with ^{64}Cu-labeled RGD-bombesin heterodimer. J Nucl Med. 2009; 50:1168–1177. [PubMed: 19525469]

27. Prasanphanich AF, Nanda PK, Rold TL, Ma L, Lewis MR, Garrison JC, Hoffman TJ, Sieckman GL, Figueroa SD, Smith CJ. [^{64}Cu-NOTA-8-Aoc- BBN(7-14)NH_2] targeting vector for positron-emission tomography imaging of gastrin-releasing peptide receptor-expressing tissues. Proc Natl Acad Sci USA. 2007; 104:12462–12467. [PubMed: 17626788]

28. Hoffman TJ, Smith CJ. True radiotracers: Cu-64 targeting vectors based upon bombesin peptide. Nucl Med Biol. 2009; 36:579–585. [PubMed: 19647163]

29. Liu D, Overbey D, Watkinson LD, Smith CJ, Figueroa SD, Hoffman TJ, Forte LR, Volkert WA, Giblin MF. Comparative evaluation of three ^{64}Cu-Labeled *E. coli* heat-stable enterotoxin analogues for PET imaging of colorectal cancer. Bioconjugate Chem. 2010; 21:1171–1176.

30. Bass LA, Wang M, Welch MJ, Anderson CJ. In vivo transchelation of copper-64 from TETA-octreotide to superoxide dismutase in rat liver. Bioconjugate Chem. 2000; 11:527–532.

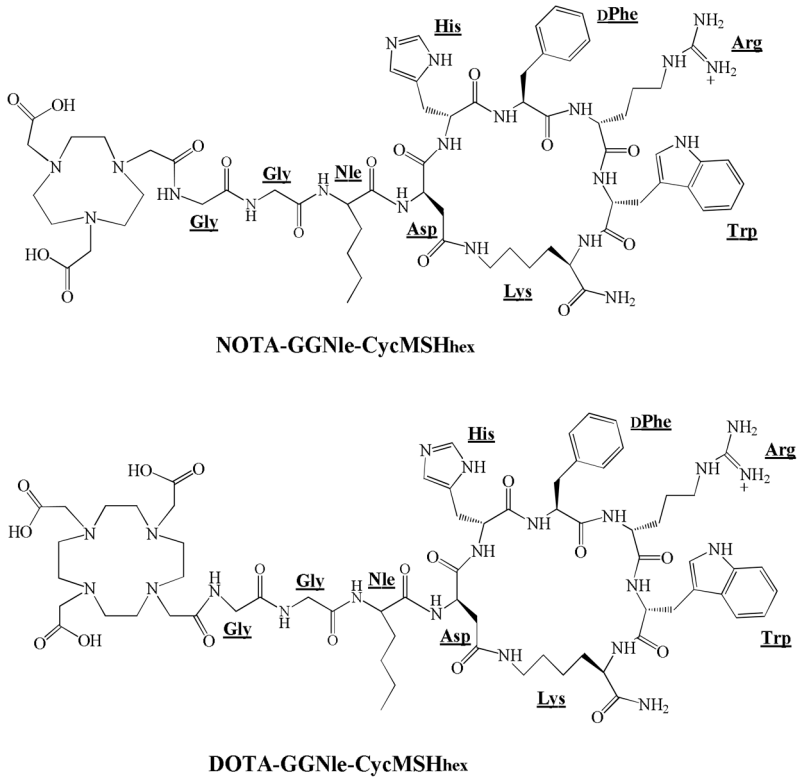

Figure 1.
Schematic structures of NOTA-GGNle-CycMSH$_{hex}$ and DOTA-GGNle-CycMSH$_{hex}$.

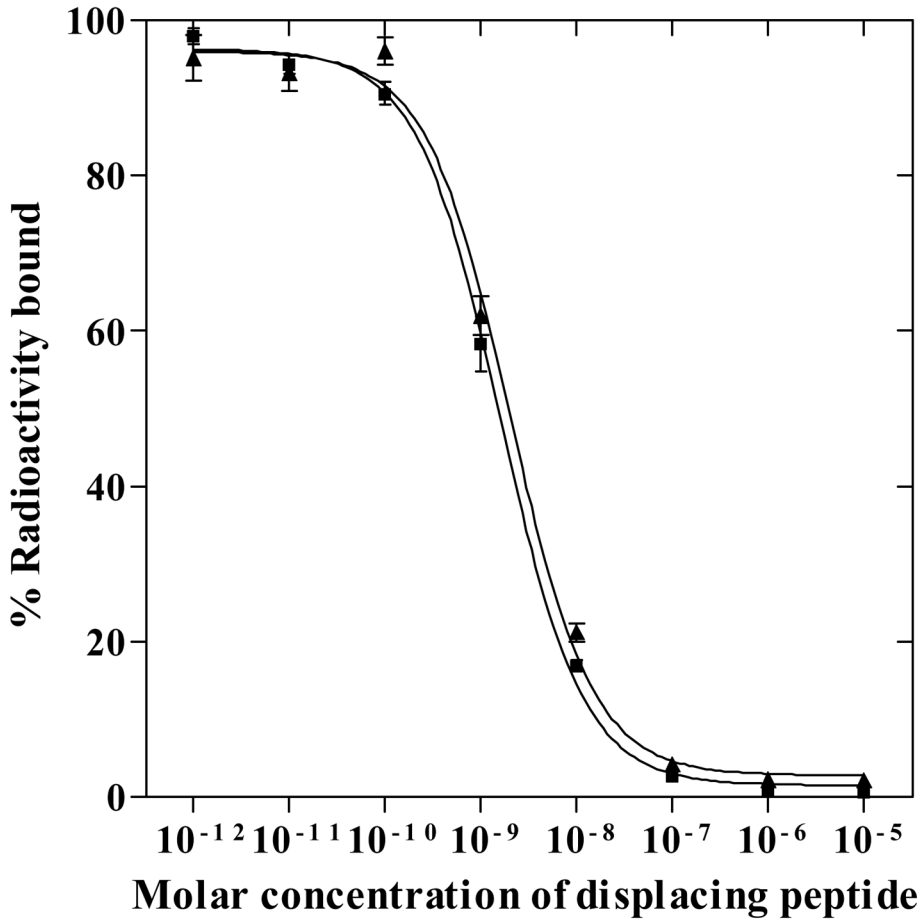

Figure 2.

The *in vitro* competitive binding curves of NOTA-GGNle-CycMSH$_{hex}$ (■) and DOTA-GGNle-CycMSH$_{hex}$ (▲) in B16/F1 melanoma cells. The IC_{50} values of NOTA-GGNle-CycMSH$_{hex}$ and DOTA-GGNle-CycMSH$_{hex}$ were 1.6 and 2.1 nM, respectively. The data of DOTA-GGNle-CycMSH$_{hex}$ was cited from our previous report23 for comparison.

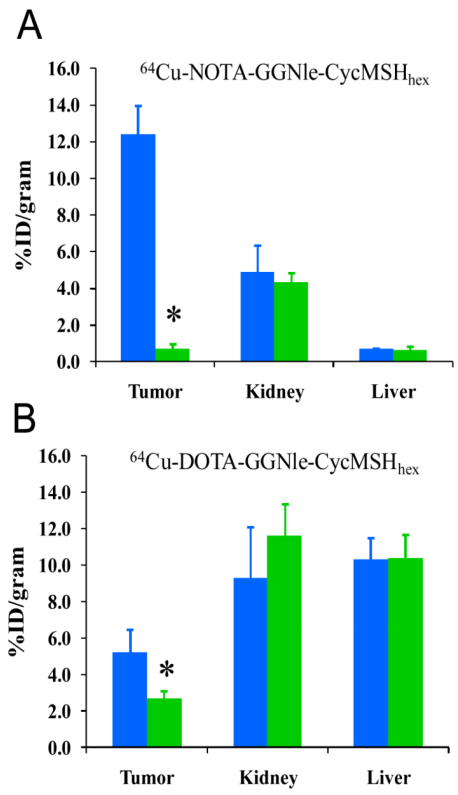

Figure 3.

The tumor, kidney and liver uptake of ^{64}Cu-NOTA-GGNle-CycMSH$_{hex}$ (A) and 64Cu-DOTA-GGNle-CycMSH$_{hex}$ (B) with (■) or without (■) 10 μg of NDP-MSH blockade at 2 h post-injection. *p<0.05.

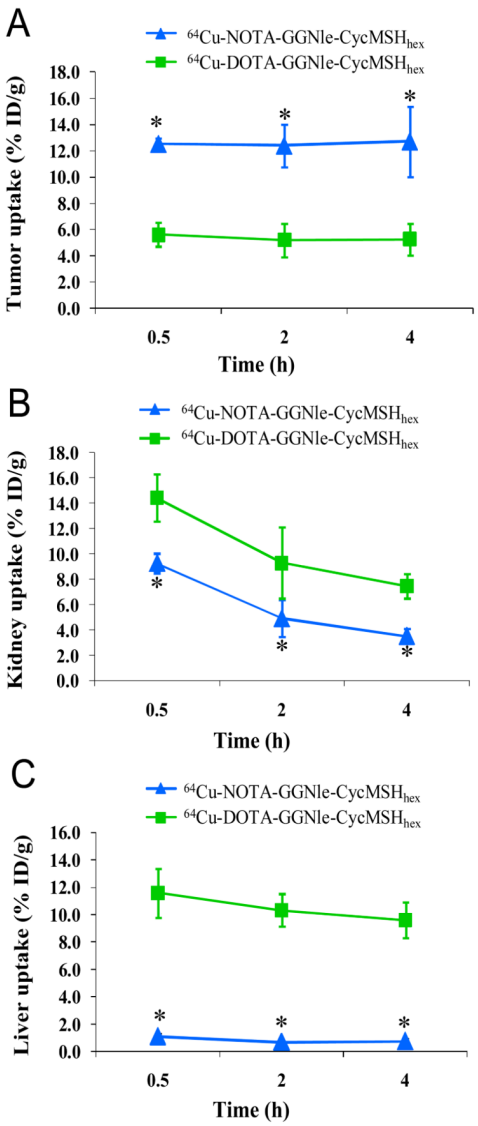

Figure 4.

The comparison of tumor (A), kidney (B) and liver (C) uptake between ^{64}Cu-NOTA-GGNle-CycMSH$_{hex}$ (▲) and ^{64}Cu-DOTA-GGNle-CycMSH$_{hex}$ (■) at 0.5, 2 and 4 h post-injection. *p<0.05.

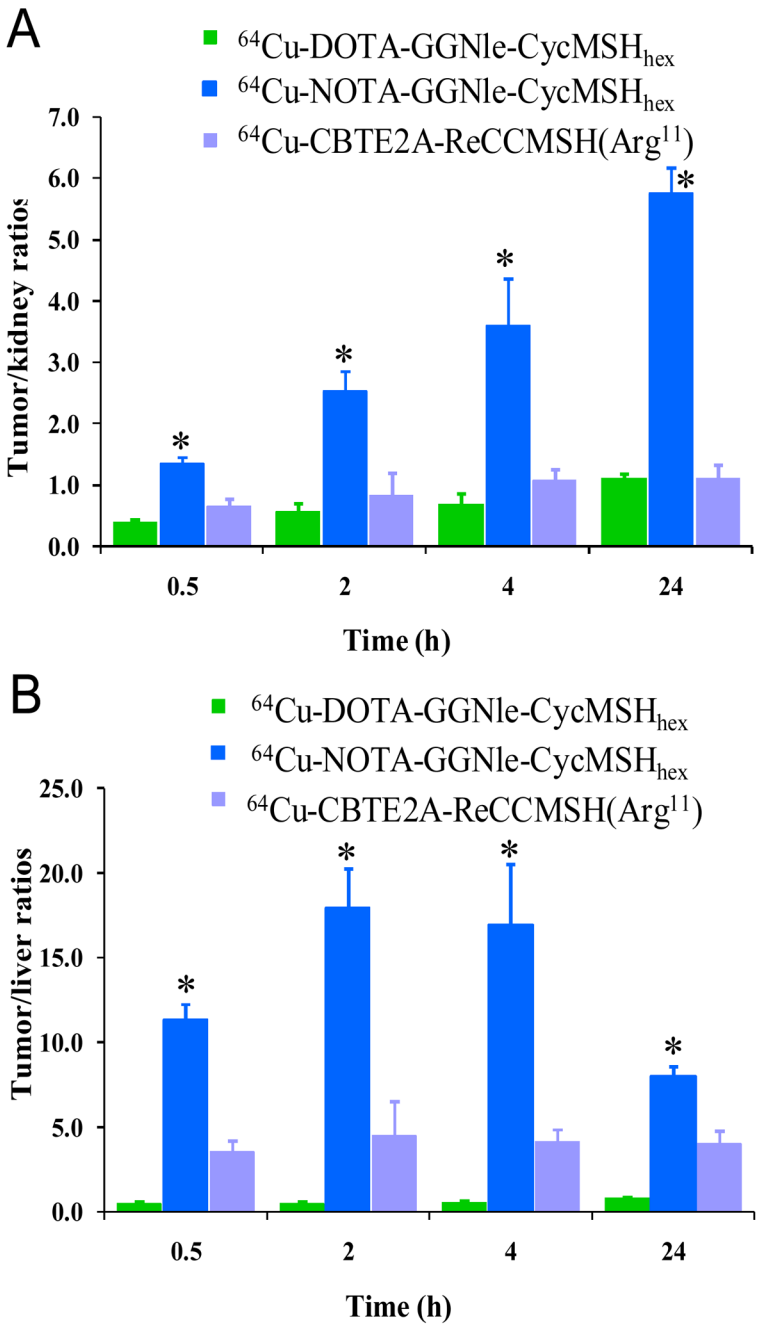

Figure 5.

The comparison of tumor/kidney (A) and tumor/liver (B) uptake ratios among ^{64}Cu-DOTA-GGNle-CycMSH$_{hex}$ (■), ^{64}Cu-NOTA-GGNle-CycMSH$_{hex}$ (■) and ^{64}Cu-CBTE2A-ReCCMSH(Arg^{11}) (■) at 0.5, 2, 4 and 24 h post-injection. *$p<0.05$, significance comparison between ^{64}Cu-NOTA-GGNle-CycMSH$_{hex}$ and 64Cu-DOTA-GGNle-CycMSH$_{hex}$, and between ^{64}Cu-NOTA-GGNle-CycMSH$_{hex}$ and 64Cu-CBTE2A-ReCCMSH(Arg11). The tumor/kidney and tumor/liver uptake ratios of ^{64}Cu-CBTE2A-ReCCMSH(Arg^{11}) (■) were calculated based on the results published by Wei et al.[14]

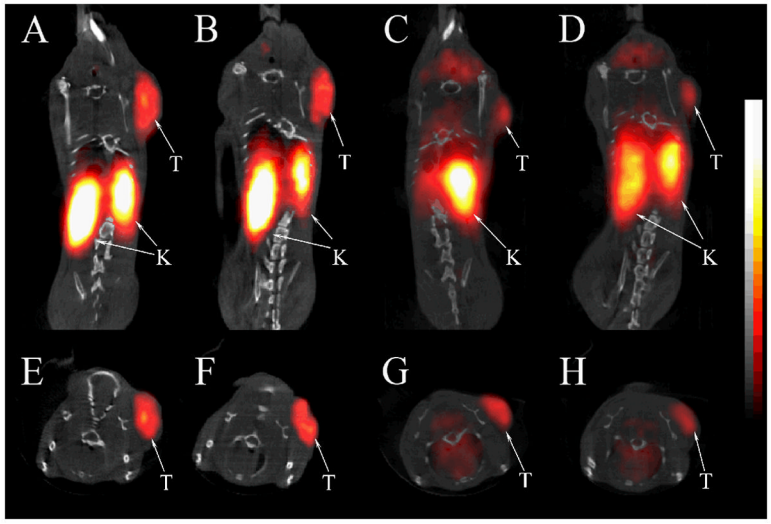

Figure 6.

Representative coronal (A, B, C, D) and transversal (E, F, G, H) PET/CT images of B16/F1 melanoma-bearing mice (12 days post cell inoculation) at 2 h (A, E, C, G) and 4 h (B, F, D, H) post-injection of 37.0 MBq of ^{64}Cu-NOTA-GGNle-CycMSH$_{hex}$ (A, B, E, F) or 64Cu-DOTA- GGNle-CycMSH$_{hex}$ (C, D, G, H). The tumors (T) and kidneys (K) were highlighted with arrows on the images.

Table 1

Biodistribution of ^{64}Cu-NOTA-GGNle-CycMSH$_{hex}$ in B16/F1 melanoma-bearing C57 mice. The data were presented as percent injected dose/gram or as percent injected dose (mean ± SD, n=5)

Tissue	0.5 h	2 h	4 h	24 h
	Percent injected dose/gram (%ID/g)			
Tumor	12.51±0.44	12.39±1.61	12.71±2.68	4.25±0.32
Brain	0.10±0.03	0.04±0.02	0.07±0.04	0.04±0.03
Blood	1.59±0.19	0.33±0.10	0.30±0.11	0.10±0.04
Heart	0.89±0.29	0.24±0.13	0.41±0.24	0.13±0.09
Lung	2.05±0.26	0.56±0.09	0.71±0.17	0.37±0.11
Liver	1.10±0.18	0.69±0.06	0.75±0.17	0.53±0.07
Spleen	0.51±0.07	0.25±0.09	0.17±0.08	0.15±0.06
Stomach	0.65±0.15	0.76±0.27	1.02±0.17	0.22±0.04
Kidneys	9.28±0.77	4.92±1.43	3.53±0.57	0.74±0.18
Muscle	0.31±0.08	0.29±0.16	0.36±0.09	0.04±0.03
Pancreas	0.71±0.04	0.29±0.13	0.34±0.04	0.30±0.14
Bone	0.41±0.19	0.27±0.05	0.19±0.06	0.09±0.07
Skin	2.23±0.21	0.35±0.11	0.71±0.21	0.35±0.27
	Percent injected dose (%ID)			
Intestines	1.27±0.11	1.41±0.70	1.19±0.23	0.50±0.20
Urine	76.82±1.19	91.67±1.57	91.47±1.66	97.05±0.55
	Tumor-to-normal-tissue uptake ratio			
Tumor/Blood	7.87	37.55	42.37	42.50
Tumor/Heart	14.06	51.63	31.00	32.69
Tumor/Kidneys	1.35	2.52	3.60	5.74
Tumor/Lung	6.10	22.13	17.90	11.49
Tumor/Liver	11.37	17.96	16.95	8.02
Tumor/Stomach	19.25	16.30	12.46	19.32
Tumor/Muscle	40.35	42.72	35.31	106.25

Table 2

Biodistribution of ^{64}Cu-DOTA-GGNle-CycMSH$_{hex}$ in B16/F1 melanoma-bearing C57 mice. The data were presented as percent injected dose/gram or as percent injected dose (mean ± SD, n=5)

Tissue	0.5 h	2 h	4 h	24 h
	Percent injected dose/gram (%ID/g)			
Tumor	5.61±0.91	5.20±1.28	5.25±1.22	5.96±0.36
Brain	0.27±0.03	0.39±0.22	0.17±0.06	0.29±0.06
Blood	2.33±0.54	1.03±0.19	0.81±0.33	1.07±0.17
Heart	2.22±0.25	1.75±0.13	1.45±0.13	2.23±0.10
Lung	3.76±0.54	3.93±0.64	4.39±0.36	4.45±0.51
Liver	11.59±1.77	10.33±1.18	9.61±1.34	7.23±0.58
Spleen	1.43±0.58	0.82±0.26	1.12±0.26	2.87±1.00
Stomach	2.83±0.84	4.78±0.96	5.09±0.69	1.21±0.14
Kidneys	14.44±1.85	9.30±2.81	7.45±0.96	5.39±0.42
Muscle	0.80±0.12	0.42±0.24	0.02±0.02	0.34±0.16
Pancreas	1.34±0.28	1.30±0.23	1.26±0.16	1.40±0.28
Bone	1.07±0.24	0.82±0.28	1.95±0.53	0.42±0.11
Skin	2.46±0.40	1.60±0.35	1.27±0.47	0.46±0.40
	Percent injected dose (%ID)			
Intestines	7.19±0.35	10.71±1.68	12.52±2.98	6.63±0.51
Urine	46.00±4.07	62.68±3.56	62.22±4.43	67.36±1.55
	Tumor-to-normal-tissue uptake ratio			
Tumor/Blood	2.41	5.05	6.48	5.57
Tumor/Heart	2.53	2.97	3.62	2.67
Tumor/Kidneys	0.39	0.56	0.70	1.11
Tumor/Lung	1.49	1.32	1.20	1.34
Tumor/Liver	0.48	0.50	0.55	0.82
Tumor/Stomach	1.98	1.09	1.03	4.93
Tumor/Muscle	7.01	12.38	262.50	17.53